Published in final edited form as:
Chem Commun (Camb). 2018 January 25; 54(9): 1097–1100. doi:10.1039/c7cc09067f.

Oxidation of a [CU$_2$S] Complex by N$_2$O and CO$_2$: Insights into a Role of Tetranuclearity in the Cu$_z$ Site of Nitrous Oxide Reductase†

Sharareh Bagherzadeh[a] and **Neal P. Mankad**[a]

[a]Department of Chemistry, University of Illinois at Chicago, 845 W. Taylor St., Chicago, IL 60607, USA

Abstract

Oxidation of a [Cu$_2$(μ-S)] complex by N$_2$O or CO$_2$ generated a [Cu$_2$(μ-SO$_4$)] product. In the presence of a sulfur trap, a [Cu$_2$(μ-O)] species also formed from N$_2$O. A [Cu$_2$(μ-CS$_3$)] species derived from CS$_2$ modeled initial reaction intermediates. These observations indicate that one role of tetranuclearity in the Cu$_z$ catalytic site of nitrous oxide reductase is to protect the crucial S^{2-} ligand from oxidation.

Because nitrous oxide (N$_2$O) is harmful as a greenhouse gas and ozone layer destroyer,[1,2] it is critical to understand the mechanisms by which nature regulates its atmospheric concentrations. Notably, during the terminal step of bacterial denitrification, N$_2$O undergoes two-electron reduction catalyzed by nitrous oxide reductase (N$_2$OR), generating benign N$_2$ + H$_2$O as products.[3] The active site for catalytic N$_2$O reduction in N$_2$OR is a tetranuclear copper cluster, Cu$_z$.[4-6] The kinetically competent form of Cu$_z$ that participates in enzymatic catalysis has a [Cu$_4$(μ$_4$-S)] structural core,[7] which activates N$_2$O upon reduction to the 4Cu^I state.[8] Computational studies indicate that the reaction coordinate for N-O cleavage involves μ-1,3 binding between two of the Cu centers, labeled Cu$_I$ and Cu$_{IV}$ (Scheme 1), with crucial assistance from hydrogen bond donation by a protonated lysine residue in the secondary coordination sphere.[9] Thus, only two Cu centers, Cu$_I$ and Cu$_{IV}$, participate directly in N$_2$O binding and reductive N-O cleavage. The other two Cu centers, Cu$_{II}$ and Cu$_{III}$, do not interact directly with the N$_2$O substrate according to this model. Furthermore, within the synthetic copper-sulfur model literature, it is clear that dicopper species are capable of mediating two-electron reduction of N$_2$O,[10-12] and thus that tetranuclearity is not a requirement for N$_2$O reduction with copper-sulfur clusters.[13] However, it should be noted that none of the synthetic copper- sulphur clusters with activity towards N$_2$O feature an unprotected S^{2-}ligand.

An intriguing question, then, is what are the roles of the “spectator” Cu$_{II}$ and Cu$_{III}$ centers in the function of N$_2$OR. In other words, why is the catalytic site of N$_2$OR tetranuclear as opposed to dinuclear if only two Cu centers are required for the two-electron reduction of

---

†Electronic Supplementary Information (ESI) available: Experimental procedures, spectral data, and crystallographic data.

Correspondence to: Neal P. Mankad.

Conflicts of interest: There are no conflicts to declare.

N_2O? Two possible roles for Cu_{II} and Cu_{III} have been proposed in the literature. First, the two electrons that ultimately transfer from Cu_z to N_2O are delocalized over all four Cu centers via the covalent μ_4-S^{2-}bridge, which serves to lower the energetic barrier for electron transfer.[9] Second, a computational study indicates that a putative [Cu_2(μ-S)] core would be susceptible to deactivation by protonation of the S^2 ligand under catalytic conditions.[14] Thus, the conventional wisdom is that while the Cu_{II} and Cu_{III} sites do not interact directly with substrate, they serve to facilitate electron transfer and to protect against protonation.

Studying the small-molecule activation chemistry of a model [Cu_2(μ-S)] complex could add further insight into possible roles of tetranuclearity in Cu_z. An excellent candidate for such studies is the complex [(IPr*)Cu]$_2$(μ-S) (**1**), which was published posthumously by Hillhouse in 2015.[15] Reactivity studies of **1** with organic substrates established the nucleophilic character of its bridging S^{2-}ligand, but no reactivity studies with small molecules such as N_2O were reported. In this study, we have examined the small-molecule activation chemistry of **1** towards N_2O and its isoelectronic analogue, CO_2. Our results lead us to propose that additional roles of tetranuclearity in Cu_Z that have not been appreciated before might include protection of the S^{2-}ligand against oxidation by N_2O and against expulsion from the active site during N_2O reduction.

Exposing **1** to N_2O (1 atm, room temperature) resulted in a mixture of six different compounds, according to ^1H NMR analysis (Scheme 1a). The major product of the reaction was found to be [(IPr*)Cu]$_2$(μ-SO_4) (**2**), which exhibits a diagnostic ^1H NMR resonance for the IPr* *para*-methyl group at 1.75 ppm (Figure 1). The identity of **2** was confirmed by generating it independently from (IPr*)CuCl + Ag_2SO_4, from observing the $[M+H]^+$ ion by ESI-MS, and by X-ray crystallography[‡] (Figure 2a). A minor product was found to be [(IPr*)Cu]$_2$(μ-O) (**3**) when the reaction was continued to >36 h; this species has a diagnostic ^1H NMR resonance at 1.78 ppm. The identity of **3** is tentatively proposed by noting that it was generated independently from the dehydration of (IPr*)CuOH[‡] by heating over molecular sieves, and from observing the $[M+H]^+$ ion by ESI-MS. We have been unable to grow X-ray quality crystals of **3** even after repeated attempts. A third species, yet unidentified, was determined to be an intermediate that converts to **2** upon further reaction with N_2O. This conclusion was reached by observing that this species, which has a diagnostic ^1H NMR resonance at 1.74 ppm (Figure 1), converted to **2** when the reaction was continued beyond 24 h to 60 h under N_2O. In contrast, no further conversion of this intermediate to **2** was evident even at 5 d when the N_2O atmosphere was replaced with N_2 at the 24-h time point. The other three components of the product mixture (1.82, 1.69, 1.68 ppm in Figure 1) have not been identified but formed in only small quantities. These three products also formed when **1** was exposed to air, but no formation of **2** or **3** from either air or O_2 was evident.

[‡] Crystal data for (IPr*)CuOH: $C_{73}H_{65}CuN_2O_2$, $M = 1065.71$, Monoclinic, $a = 12.7160(14)$, $b = 18.419(2)$, 24.254(2) Å, $\beta = 92.238(3)°$, $V = 5676.3(10)$ Å^3, $T = 100$ K, $P2_1/c$, $Z = 4$, 9141 reflection measured, 7300 unique, ($R_{int} = 0.0583$), $wR(F^2) = 0.099$ (all data). Crystal data for **2**: $C_{163}H_{164}Cu_2N_4O_8S$, $M = 2232.60$, Triclinic, $a = 22.1927(19)$, $b = 22.3352(19)$, 26.585(2) Å, $\alpha = 103.713(2)$, $\beta = 92.238(3)$, $\gamma = 90.105(2)°$, $V = 12202.4(18)$ Å^3, $T = 100$ K, P-1, $Z = 4$, 35056 reflection measured, 16177 unique, ($R_{int} = 0.3306$), $wR(F^2) = 0.4568$ (all data). Crystal data for **4**: $C_{158.50}H_{154}Cu_2N_4S_3$, $M = 2200.99$, Monoclinic, $a = 26.864(10)$, $b = 28.131(11)$, 18.999(7) Å, $\beta = 90°$, $V = 14358(9)$, $T = 293$ K, $C2/c$, $Z = 4$, 17085 reflection measured, 7281 unique, ($R_{int} = 0.2106$), $wR(F^2) = 0.2875$ (all data).

Interestingly, when N_2O was added to a mixture of **1** and PPh_3, the products **2** and **3** formed in roughly equimolar amounts products rather than **2** being the major product (Scheme 2b). The formation of Ph3P=S was detected by ^{31}P NMR analysis, indicating that the byproduct of **1** + N_2O converting to **3** is likely elemental sulfur. It is important to note that no reaction was observed between **1** and PPh_3 under N_2, and that $Ph_3P{=}S$ was not observed when PPh_3 was added to the product mixture after 24 h of exposing **1** to N_2O as opposed to having PPh_3 present from the beginning.

Exposing **1** to CO_2 (1 atm, room temperature) provided similar results to the N_2O reaction (Scheme 2a). Once again, the major product was **2**. The same three unidentified byproducts formed in small quantities, although no obvious intermediate was observed. An additional minor product was the (IPr*)-CO_2 adduct, whose identity was established by independently exposing the free IPr* carbene to CO_2 (1 atm, room temperature) as is well known for related carbenes.[16] Unlike in the N_2O case, the presence of PPh_3 in the reactant mixture did not impact the nature of the product distribution, and neither compound **3** nor $Ph_3P{=}S$ were observed from CO_2 under any conditions we examined.

To gain insight into the initial interaction between **1** and N_2O/CO_2, we examined the reactivity of **1** with CS_2 as a model substrate. A rapid reaction was observed between **1** and CS_2, generating pink-colored $[(IPr^*)Cu]_2(\mu\text{-}CS_3)$ (**4**) quantitatively (Scheme 2c). The identity of **4** was confirmed by X-ray crystallography[‡] (Figure 2b) and by observation of the $[M+H]^+$ ion by ESI-MS. Using the structure of **4** as a starting point, we were able to optimize the structure of a DFT model, $[(IMe)Cu]_2(\mu\text{-}CS_3)$ (**4′**), whose $[Cu_2CS_3]$ core closely resembles the experimentally determined structure of **4** (IMe = *N,N′*-dimethylimidazol-2-ylidene). Then, using the **4′** structure as a starting point, we located energy minima for the DFT models $[(IMe)Cu]_2(\mu\text{-}SCO_2)$ (**5′**) and $[(IMe)Cu]_2(\mu\text{-}SN_2O)$ (**6′**), which are shown in Figure 3. Unlike **4′**, the **5′** and **6′** structures exhibit unsymmetrical bridging within the dicopper core. In both cases, one Cu center is engaging in Lewis acid activation of an oxygen atom from the small molecule, with multiple bond character being evident from the optimized C-O/N-N bond distances distal to this Lewis acid activation. Loss of CO and N_2 from **5′** and **6′**, respectively, would generate $[(IMe)Cu]_2(\mu\text{-}SO)$ (**7′**), which we also were able to optimize (Figure 3). The optimized structure of **7′** places the sulfur and oxygen centers clearly within bonding distance (1.80 Å) and features an unsymmetrical, puckered $[Cu_2(\mu\text{-}SO)]$ core. We propose that **7′** is a reasonable approximation for an early intermediate that ultimately is either exhaustively oxidized by the small-molecule oxidant to generate **2** or trapped by PPh_3 to generate **3**.

Based on the experimental and computational observations outlined above, our preliminary mechanistic proposal is outlined in Scheme 3. Initial insertion of the small-molecule heteroallene into a Cu-S bond of **1** produces intermediate **A**, which in turn evolves N_2 or CO to generate intermediate **B**. From here, presumably there are two distinct pathways. One involves further oxidation of **B** by three sequential equivalents of the heteroallene oxidant to produce **2**. The other involves reversible expulsion of elemental sulfur to produce **3**. In the case of N_2O, the formation of **3** can be accelerated by trapping the elemental sulfur with PPh_3. In the case of CO_2, the formation of **2** is sufficiently rapid that **3** does not form even in the presence of PPh_3. Further studies will be required to understand the conversion of **A** to **B** and to elucidate how **B** is further oxidized by N_2O and CO_2.

These studies reveal the chemistry of a $[Cu_2(\mu_2\text{-}S)]$ core towards small molecules including N_2O. If one were to imagine the catalytic site of N_2OR having such a dinuclear core instead of a tetranuclear $[Cu_4(\mu_4\text{-}S)]$ core, productive catalysis would be hampered or prevented by oxidation and/or expulsion of the S^{2-}ligand. Thus, in addition to participating in electron delocalization and preventing protonolysis, another role of the two “spectator” Cu centers in Cu_z may be to prevent these unproductive side reactions of the bridging S^{2-}ligand from competing with productive N_2O reductase reactivity. In this context, it is intriguing to note that a “protected” tricopper analogue of **1**, $\{[(IPr)Cu]_3(\mu_3\text{-}S)\}+$ (**5**),[17] was found to be inert towards N_2O and CO_2 under conditions where **1** undergoes the reactions described in this manuscript (Scheme 2d).

Supplementary Material

Refer to Web version on PubMed Central for supplementary material.

Acknowledgments

Funding was provided by NIH/NIGMS (R01 GM116820). DFT calculations were performed at the UIC Extreme Computing facility. Dr. Cina Foroutan-Nejad provided useful suggestions on DFT calculations. Prof. Don Wink assisted with X-ray crystallography. We are grateful for inspiration provided by research of the late Prof. Gregory Hillhouse.

Notes and references

1. Thomson AJ, Giannopoulos G, Pretty J, Baggs EM, Richardson DJ. Philos Trans R Soc Lond, B, Biol Sci. 2012; 367:1157–1168. [PubMed: 22451101]
2. Ravishankara AR, Daniel JS, Portmann RW. Science. 2009; 326:123–125. [PubMed: 19713491]
3. Pauleta SR, Dell'Acqua S, Moura I. Coord Chem Rev. 2013; 257:332–349.
4. Brown K, Tegoni M, Prudêncio M, Pereira AS, Besson S, Moura JJ, Moura I, Cambillau C. Nat Struct Biol. 2000; 7:191–195. [PubMed: 10700275]
5. Pomowski A, Zumft WG, Kroneck PMH, Einsle O. Nature. 2011; 477:234–237. [PubMed: 21841804]
6. Solomon EI, Heppner DE, Johnston EM, Ginsbach JW, Cirera J, Qayyum M, Kieber-Emmons MT, Kjaergaard CH, Hadt RG, Tian L. Chem Rev. 2014; 114:3659–3853. [PubMed: 24588098]
7. Johnston EM, Dell'Acqua S, Ramos S, Pauleta SR, Moura I, Solomon EI. J Am Chem Soc. 2014; 136:614–617. [PubMed: 24364717]
8. Ghosh S, Gorelsky SI, Chen P, Cabrito I, Moura I, Solomon EI. J Am Chem Soc. 2003; 125:15708–15709. [PubMed: 14677937]
9. Johnston EM, Carreira C, Dell'Acqua S, Dey SG, Pauleta SR, Moura I, Solomon EI. J Am Chem Soc. 2017; 139:4462–4476. [PubMed: 28228011]
10. Bar-Nahum I, Gupta AK, Huber SM, Ertem MZ, Cramer CJ, Tolman WB. J Am Chem Soc. 2009; 131:2812–2814. [PubMed: 19206272]
11. Esmieu C, Orio M, Torelli S, Le Pape L, Pécaut J, Lebrun C, Ménage S. Chem Sci. 2014; 5:4774–4784.
12. Tsai ML, Hadt RG, Vanelderen P, Sels BF, Schoonheydt RA, Solomon EI. J Am Chem Soc. 2014; 136:3522–3529. [PubMed: 24524659]
13. For N_2O reduction by a $[Cu_4(\mu_4\text{-}S)]$ model complex, see: Johnson BJ, Antholine WE, Lindeman SV, Graham MJ, Mankad NP. J Am Chem Soc. 2016; 138:13107–13110.

14. Gorelsky SI, Ghosh S, Solomon EI. J Am Chem Soc. 2006; 128:278–290. [PubMed: 16390158]

15. Zhai J, Filatov AS, Hillhouse GL, Hopkins MD. Chem Sci. 2016; 7:589–595. [PubMed: 28791108]

16. Holbrey JD, Reichert WM, Tkatchenko I, Bouajila E, Walter O, Tommasi I, Rogers RD. Chem Commun. 2002:28–29.

17. Zhai J, Hopkins MD, Hillhouse GL. Organometallics. 2015; 34:4637–4640.

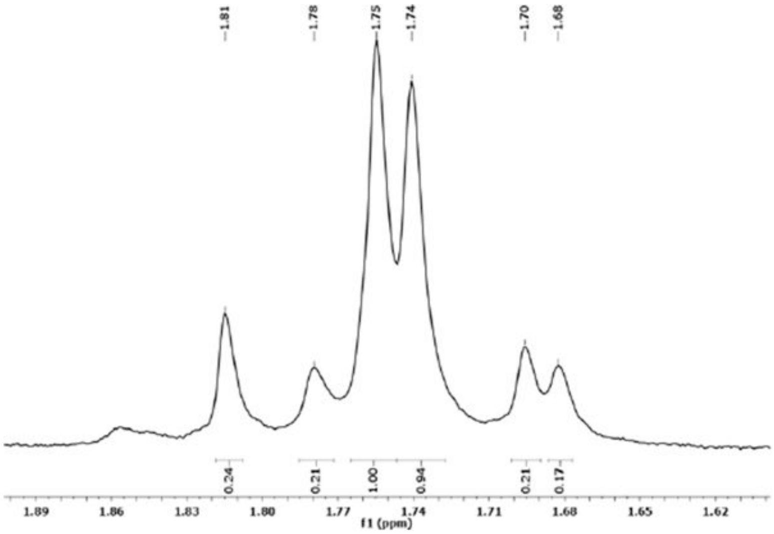

Figure 1.

The poro-methyl region of the ^{1}H NMR spectrum from reaction of **1** and N_2O (1 atm) in the absence of PPh_3

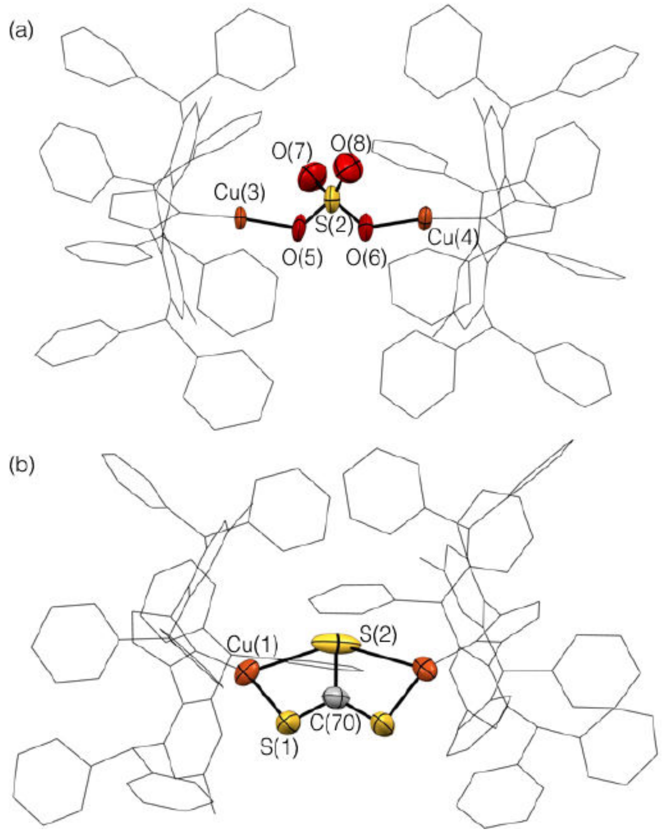

Figure 2.

Solid-state structures of (a) [(IPr*Cu)$_2$]([μ-SO$_4$) **(2)** and (b) [(IPr*)Cu)$_2$](μ-CS$_3$) (**4**) determined by X-ray crystallography. The IPr* ligands are shown as wireframes, the inorganic cores are shown as 50%-probability thermal ellipsoids, hydrogens are omitted, and only one of two molecules from the asymmetric unit of 2 is shown. Selected bond distances (Å) and angles (°) for **2**: Cu(3)-O(5), 1.937(11); Cu(4)-O(6), 1.883(10); S(2)-O(5), 1.444(12); S(2)-O(6), 1.479(12); S(2)- O(7), 1.454(14); S(2)-O(8), 1.488(14). For **4**: Cu(1)-S(1), 2.1627(17); Cu(1)-S(2), 2.905(2); S(1)-C(70), 1.677(4); S(2)-C(70), 1.708(7); S(1)-C(70)-S(2), 119.4(2); S(1)- C(70)-S(1#), 121.1(4).

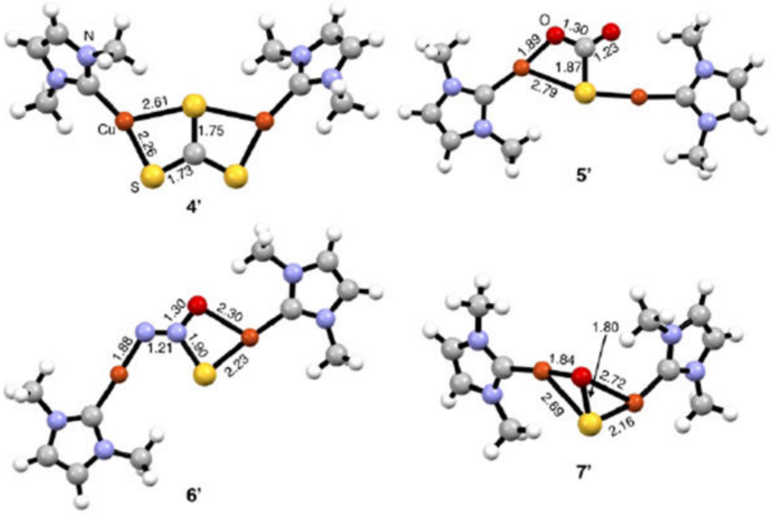

Figure 3.

DFT-optimized structures (BVP86/LANL2TZ(f)/6-311+(d)) of dicopper complexes relevant to the small-molecule activation chemistry of $[(\mathrm{IPr}^*)\mathrm{Cu}]_2(\mu\text{-S})$. Bond distance labels are in units of Å.

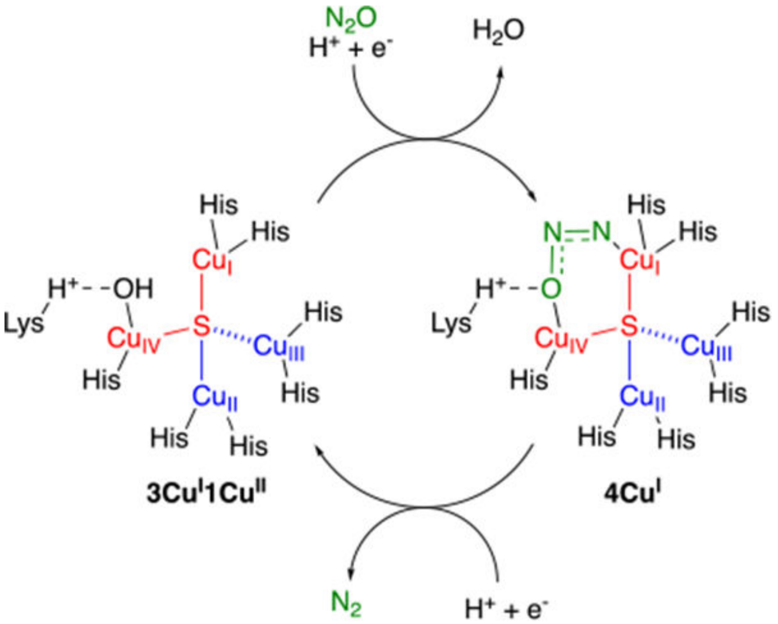

Scheme 1.
N_2O reduction at Cu_Z.

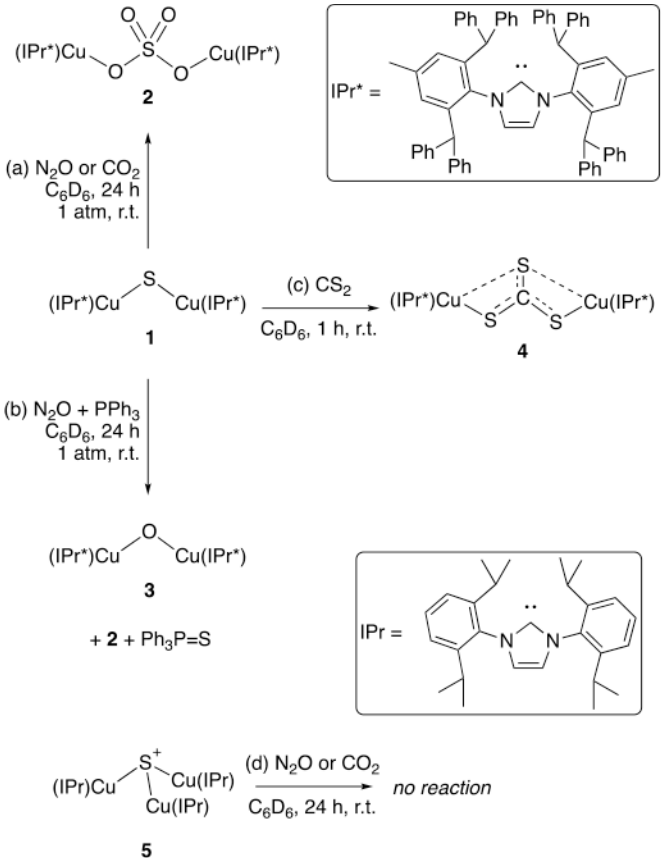

Scheme 2.

Small molecule activation experiments with $[(\mathrm{IPr}^*)\mathrm{Cu}]_2(\mu\text{-S})$ (**1**) and $\{[(\mathrm{IPr})\mathrm{Cu}]_2(\mu_3\text{-S})\}\{\mathrm{BF}_4\}$ (**5**).

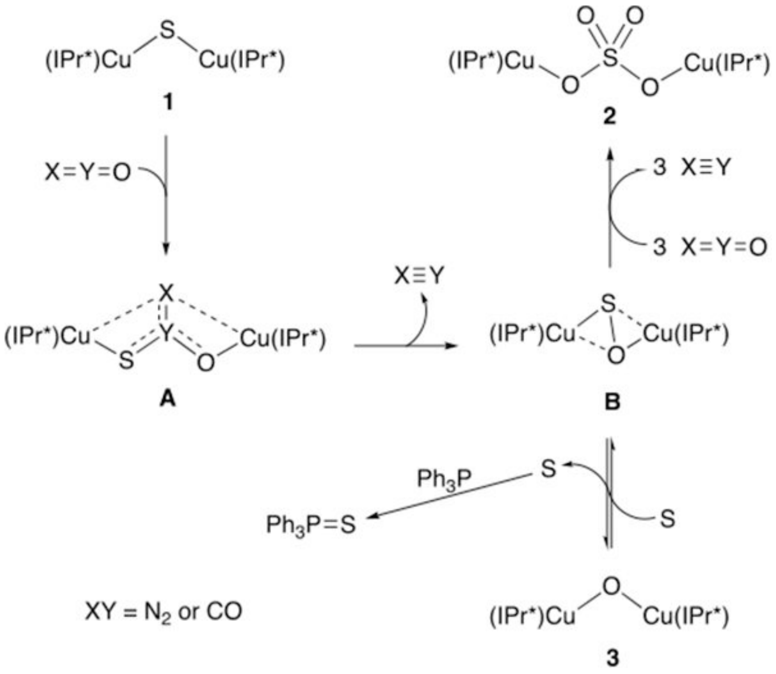

Scheme 3.

Hypothetical mechanism.